Vol. 29 (1998) *ACTA PHYSICA POLONICA B* No 12

LUTTINGER-LIQUID PHENOMENOLOGY FOR HIGH-T_c SUPERCONDUCTORS* **

K. Byczuk

Institute of Theoretical Physics, Warsaw University
Hoża 69, 00-681 Warszawa, Poland

J. Spałek

Institute of Physics, Jagiellonian University, Reymonta 4
30-059 Kraków, Poland

and W. Wójcik

Institute of Physics, Technical University
Podchorążych 1, 30-084 Kraków, Poland

(Received December 7, 1998)

Universal scaling with temperature of the resistivity and optical conductivity in the normal state follows from the time-reversal symmetry assumed for the Green function with branch cuts combined with charge-spin separation. The density of states reproduces the extended van Hove singularity in a planar system. The single-particle tunneling conductivity in the superconducting state is nonzero at zero bias voltage, reproducing the pseudogap character of the density of states in the superconducting phase even for the s-wave symmetry of the order parameter. The form of the Ginzburg–Landau functional is also provided.

PACS numbers: 74.72.–h, 71.10.Pm

1. Introduction

Landau–Fermi liquid theory was the most important concept in the physics of interacting fermions in the last forty years [1]. This theory was applied to many systems of strongly interacting fermionic particles, among them to metals, liquid ^{3}He, or even to neutron stars and quark-gluon plasma [2].

* Presented at the XXXVIII Cracow School of Theoretical Physics, Zakopane, Poland, June 1–10, 1998.
** The work supported by KBN Grant No. 2P03B 129 12.

Nowadays, there is an agreement among physicists that high-temperature copper-oxide superconductors do not belong to the class of systems whose a low-energy excitation spectrum is described by the standard Fermi-liquid theory [3]. In the discussion of electronic properties of high temperature superconductors the Marginal-Fermi-Liquid (MFL) [4] and the tomographic Anderson–Luttinger-Liquid (ALL) [5] states are invoked as alternative quantum phases describing their normal state. In these pictures a different form of the single-particle Green function is assumed at the start. The phenomenological MFL approach being very close to experiment provides an appealing picture. The basic question is whether the same type of phenomenology is possible within ALL picture, which is derived from a single basic assumption concerning the nature of this quantum liquid. In this contribution we provide such a single principle, on the basis of which we derive the explicit form of the single-particle Green function and subsequently, carry out the calculations of basic normal and superconducting properties for a planar system. Namely, we combine the electron-hole symmetry with the charge-spin separation. These two features have been discussed separately by Anderson and coworkers [5–7]. Here we decompose the properties coming from an anomalous exponent in the Green function from those due to the charge-spin separation; the emerging picture allows for a direct analysis of experiment.

2. The model and the selected physical properties of high-T_c systems

By Anderson–Luttinger quantum liquid we understand the system, single particle Green function of which has the branch cuts and, additionally, there is a charge-spin separation in the excitation spectrum. These two characteristics are combined together through the following choice of the retarded Green function

$$G_R(\boldsymbol{k},\omega) = \frac{g(\beta,\gamma)\mathrm{e}^{i\phi}}{\omega_c^{1-\beta-\gamma}(\omega-\varepsilon^c_{\boldsymbol{k}}+i0^+)^{\beta}(\omega-\varepsilon^s_{\boldsymbol{k}}+i0^+)^{\gamma}}\,, \tag{1}$$

where the dispersion relations $\varepsilon^c_{\boldsymbol{k}} = \varepsilon^c_{\boldsymbol{k}} - \mu$ and $\varepsilon^s_{\boldsymbol{k}} = \varepsilon^s_{\boldsymbol{k}} - \mu$, represent the energies of charge and spin density excitations, respectively. In part of the calculations we assume that their form is: $\varepsilon^{c,s}_{\boldsymbol{k}} = v^{c,s}_{\mathrm{F}}|\boldsymbol{k}-\boldsymbol{k}_{\mathrm{F}}| \equiv v^{c,s}_{\mathrm{F}}k \equiv (1\pm\delta)v_{\mathrm{F}}k$, where δ is called the charge-spin separation, and v_{F} is the bare Fermi velocity. The function $g(\beta,\gamma)$ is a normalization factor to be determined later. ϕ is an arbitrary phase factor. The cut-off ω_c limits the form (1) validity to the low-energy regime. Note also that the choice (1) comprises Fermi-liquid regime for $\beta=\gamma=1/2$, and $\delta=0$.

We determine the imaginary part of $G_R(\boldsymbol{k},\omega)$, which has a physical meaning of the spectral density function $A(\boldsymbol{k},\omega)$, by decomposing $G_R(\boldsymbol{k},\omega)$

into four parts: The first with $\omega > \varepsilon^c_{\boldsymbol{k}}$ and $\varepsilon^s_{\boldsymbol{k}}$, the second with $\omega < \varepsilon^c_{\boldsymbol{k}}$ and $\omega > \varepsilon^s_{\boldsymbol{k}}$, *etc.* In effect, we have

$$\begin{aligned} G(\boldsymbol{k},\omega) &= \frac{N}{|\omega-\varepsilon^c_{\boldsymbol{k}}|^\beta|\omega-\varepsilon^s_{\boldsymbol{k}}|^\gamma}\Big(\theta(\omega-|1\varepsilon^c_{\boldsymbol{k}})\theta(\omega-\varepsilon^s_{\boldsymbol{k}})+\theta(\varepsilon^c_{\boldsymbol{k}}-\omega)\theta(\omega-\varepsilon^s_{\boldsymbol{k}})\mathrm{e}^{i\pi\beta} \\ &\quad +\theta(\omega-\varepsilon^c_{\boldsymbol{k}})\theta(\varepsilon^s_{\boldsymbol{k}}-\omega)\mathrm{e}^{i\pi\gamma}+\theta(\varepsilon^c_{\boldsymbol{k}}-\omega)\theta(\varepsilon^s_{\boldsymbol{k}}-\omega)\mathrm{e}^{i\pi(\beta+\gamma)}\Big) \\ &\equiv \mathrm{Re}\,G + i\mathrm{Im}\,G\,, \end{aligned} \tag{2}$$

where $N \equiv g/\omega_c^{1-\beta-\gamma}$, and $\theta(x)$ is the step function. At this point we make a fundamental assumption, namely, the spectral density function $A(\boldsymbol{k},\omega) \equiv -(1/\pi)\mathrm{Im}\,G_R(\boldsymbol{k},\omega)$, is assumed symmetric with respect to the time reversal [8]; in the energy-momentum representation it takes the form of electron–hole symmetry, *i.e.* $A(\boldsymbol{k},\omega) = A(-\boldsymbol{k},-\omega)$. This restriction leads to the relations: $\sin\phi = \sin(\phi-\pi(\beta+\gamma))$, and $\sin(\phi-\pi\gamma) = \sin(\phi-\pi\beta)$, or explicitly to: $\pi\gamma = \pi\beta+2\pi k$, with $k = 0, \pm1, \pm2$, *etc.* Since the complex quantities are defined on the first Riemann sheet, we put $k = 0$, and thus $\beta = \gamma$. Defining $\gamma = \beta \equiv 1/2-\alpha$, we obtain the explicit form of G_R:

$$G_R(\boldsymbol{k},\omega) = \frac{g(\alpha)\mathrm{e}^{-i\pi\alpha}}{\omega_c^{2\alpha}(\omega-\varepsilon^c_{\boldsymbol{k}}+i0^+)^{\frac{1}{2}-\alpha}(\omega-\varepsilon^s_{\boldsymbol{k}}+i0^+)^{\frac{1}{2}-\alpha}}\,. \tag{3}$$

The Green function has anomalous scaling properties accounted for by two parameters: The exponent α, and by the charge-spin-separation $\delta > 0$. For $\alpha = 0$ and $\delta \neq 0$ we obtain the liquid with the Fermi-liquid scaling $G(\Lambda\boldsymbol{k},\Lambda\omega) = \Lambda^{-1}G(\boldsymbol{k},\omega)$, which was obtained before [9] within the bosonization scheme in d dimensions by taking into account a singular forward scattering amplitude. In what follows α and $v_{\mathrm{F}}^{c,s} = (1\pm\delta)v_{\mathrm{F}}$ are regarded as parameters to be determined from the comparison with experiment. The form (3) is symmetric with respect to interchange of the charge and the spin components ($v_{\mathrm{F}}^c \leftrightarrow v_{\mathrm{F}}^s$), as we expect that the charge-excitation spectrum is transformed into the spin counterpart upon the sign reversal of the singular part of the interaction (*i.e.* the change of δ sign) [9].

The spectral density is of the following explicit form

$$\begin{aligned} A(\boldsymbol{k},\omega) &= \frac{g(\alpha)}{\pi\omega_c}\left\{\frac{\sin(\pi\alpha)\,(\theta(\omega-\varepsilon^c_{\boldsymbol{k}})\theta(\omega-\varepsilon^s_{\boldsymbol{k}})+\theta(\varepsilon^c_{\boldsymbol{k}}-\omega)\theta(\varepsilon^s_{\boldsymbol{k}}-\omega))}{|\omega-\varepsilon^c_{\boldsymbol{k}}|^{\frac{1}{2}-\alpha}|\omega-\varepsilon^s_{\boldsymbol{k}}|^{\frac{1}{2}-\alpha}}\right. \\ &\quad \left. +\frac{(\theta(\omega-\varepsilon^c_{\boldsymbol{k}})\theta(\varepsilon^s_{\boldsymbol{k}}-\omega)+\theta(\varepsilon^c_{\boldsymbol{k}}-\omega)\theta(\omega-\varepsilon^s_{\boldsymbol{k}}))}{|\omega-\varepsilon^c_{\boldsymbol{k}}|^{\frac{1}{2}-\alpha}|\omega-\varepsilon^s_{\boldsymbol{k}}|^{\frac{1}{2}-\alpha}}\right\}. \end{aligned} \tag{4}$$

It has the scaling property $A(\Lambda\boldsymbol{k},\Lambda\omega) = \Lambda^{-(1-2\alpha)}A(\boldsymbol{k},\omega)$ and differs slightly from that in [10], as our form is explicitly symmetric with respect to charge and spin excitations.

2.1. Electrical resistivity

With the help of Green function (3) we can obtain the fundamental scaling of the resistivity in the whole temperature range. Explicitly, the static conductivity can be obtained from the Kubo formalism; the corresponding formula without vertex corrections [7] can be written as

$$\sigma = \sigma_0 \int\limits_{-\omega_c/2}^{\omega_c/2} d\omega \, (-\frac{\partial f}{\partial \omega}) \int\limits_{-\omega_c/2}^{\omega_c/2} d\omega' \, [A(\omega', \omega)]^2 \,, \tag{5}$$

where σ_0 is of the order of e^2/h, $A(\omega', \omega) \equiv A(k = \omega'/v_\mathrm{F}, \omega)$, $f(\omega) = [\exp(\beta\omega) + 1]^{-1}$, and $\beta = (k_\mathrm{B}T)^{-1}$ is the inverse temperature. By changing the variables $\omega \to \beta\omega$, $\omega' \to \beta\omega'$, we obtain the scaling $\sigma \sim T^{-1+4\alpha}$ for $\omega_c\beta \to \infty$. Hence, the resistivity $\rho(T)$ scales as $T^{1-4\alpha}$. This means that at the optimal doping the exponent α should be small. In the terms of our microscopic approach [9] it means that the divergence of the forward scattering amplitude is sufficient to explain the situation with $\alpha = 0$. In other words, the dependence $\rho \sim T$ can be explained solely on the basis of charge-spin separation. One should note that for $\alpha = 0$ the distribution function has a step at k_F, as in the Fermi-liquid phase and is called [11] the case with the Fermi-liquid scaling. Also, in (5) we have a one-dimensional integration over ω', a specific feature of the tomographic nature of ALL, and of the fact that $\varepsilon_{\boldsymbol{k}} \sim k$.

One can also define the frequency dependent conductivity as

$$\sigma(\omega) \sim \int\limits_{-\omega_c\beta/2}^{\omega_c\beta/2} d\varepsilon \, (\frac{f(\varepsilon) - f(\varepsilon + \omega)}{\omega}) \int\limits_{-\omega_c\beta/2}^{\omega_c\beta/2} d\omega' \, A(\omega', \omega + \varepsilon) A(\omega', \omega) \,, \tag{6}$$

and the transport relaxation time

$$\tau_\mathrm{tr}(\omega) = \int\limits_{-\omega_c\beta/2}^{\omega_c\beta/2} d\omega' \, [A(\omega', \omega)]^2 \sim \omega^{-1+4\alpha} \,. \tag{7}$$

To illustrate the derived temperature dependences of transport properties we have shown in Fig. 1 the frequency dependent conductivity $\sigma(\omega)$. This quantity has a hump at intermediate frequencies for $\alpha \geq 0.1$ that may be identified with the so-called mid-infrared band [12]. Also, the system approaches a nonmetallic behavior for $T \to 0$ when $\alpha > 1/4$. The numerical results have been performed for a constant (equal to $1/\omega_c$) form of the density of states. The choice of the density of states should not be crucial, since the transport characteristics involve integrations over ω.

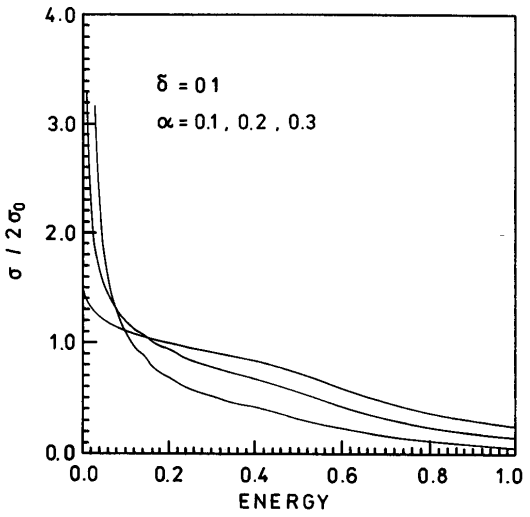

Fig. 1. Frequency dependent conductivity in units of $2e^2/h$, for various values of α and $\delta = 0.1$.

2.2. Density of states

An important characteristic is the density of states, which in two dimensions is calculated by an integration over the Brillouin zone, *i.e.*

$$\rho(\omega) \equiv \frac{2}{(2\pi)^2} \int d^2k \, A(\boldsymbol{k}, \omega) \, . \tag{8}$$

This integral has been performed taking a realistic dispersion relation: $\varepsilon_{\boldsymbol{k}}^{c,s} = (1 \pm \delta)(-0.5(\cos k_x + \cos k_y) + t_1 \cos k_x \cos k_y)$, *i.e.* including the second-neighbor hopping t_1. In Fig. 2 we have displayed the results for $t_1 = 0.2$, and different values of δ (all energies are in units of ω_c). They reproduce the form determined experimentally [13] with the extended van Hove singularity. These calculations did not require a complicated form of the dispersion relation usually taken to reproduce this feature, but ascribe it to the many-body nature of excitations [14].

On the basis of the form of $A(\boldsymbol{k}, \omega)$ and $\rho(T, \omega)$ one can specify the *fundamental* regimes:

(*i*) $\alpha \to 1/2$, where the spectrum becomes totally incoherent, *i.e. the localization threshold is reached*;

(*ii*) $1/2 > \alpha > 1/4$, where $\rho(T \to 0) \to \infty$, *i.e. the underdoped regime*;

(*iii*) $0 \leq \alpha < 1/4$, where the system is *metallic*.

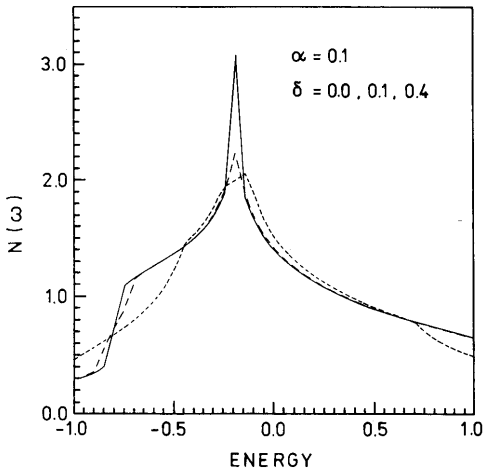

Fig. 2. Density of states in the normal state.

$\rho(T) \sim T$ for $\alpha = 0$ and $\delta \neq 0$. This ALL state terminates at a *quantum critical point* $\alpha = \delta = 0$, where the system transforms to a Landau Fermi liquid (LFL), since in that limit the Green function (1) has only single poles. Note that in the $\alpha \to 0$ limit spectral density (4) *does not* reduce adiabatically to that for LFL. This is also the reason why the conductivities (5) and (6) do not reduce respectively to the Baber and the Drude forms in that limit. Briefly, LFL constitutes a separate universality class, as it has different scaling properties and the exponents near the (critical) point $T = 0$. This is the most important qualitative feature of this work.

2.3. Gap equation and spectral density in SC phase

In order to describe the superconducing (SC) phase we make the assumption that the normal and the anomalous Green functions satisfy the BCS-like Dyson equation [5], *i.e.* can be combined into the resultant quantity $\boldsymbol{G}_R$ of the form

$$\boldsymbol{G}_R(\boldsymbol{k},\omega)^{-1} = \begin{pmatrix} G_R(\boldsymbol{k},\omega)^{-1} & \Delta_{\boldsymbol{k}} \\ \Delta^*_{\boldsymbol{k}} & (G_R(\boldsymbol{k},\omega)^{-1})^\dagger \end{pmatrix}, \tag{9}$$

where $\Delta_{\boldsymbol{k}}$ is a superconducting order parameter. This function $\boldsymbol{G}_R$ has single poles at the excitation energies

$$\omega = \pm E_{\boldsymbol{k}} \equiv \pm\sqrt{\frac{(\varepsilon^c_{\boldsymbol{k}})^2 + (\varepsilon^s_{\boldsymbol{k}})^2}{2} + \sqrt{\left(\frac{(\varepsilon^c_{\boldsymbol{k}})^2 - (\varepsilon^s_{\boldsymbol{k}})^2}{2}\right)^2 + |\tilde{\Delta}_{\boldsymbol{k}}|^4}}, \tag{10}$$

where the effective gap is

$$|\tilde{\Delta}_{\boldsymbol{k}}| = |\Delta_{\boldsymbol{k}}| \left(\frac{|\Delta_{\boldsymbol{k}}|}{\omega_c}\right)^{\frac{2\alpha}{1-2\alpha}}. \tag{11}$$

For $\alpha = \delta = 0$ this equation reduces to the BCS result. For an arbitrary α one can calculate the spectral function $A(\boldsymbol{k},\omega)$ and other characteristics. The calculation of $A(\boldsymbol{k},\omega)$ must be performed separately for $\alpha \neq 0$ and $\alpha = 0$. For $\alpha = 0$ it takes the form

$$A(\boldsymbol{k},\omega) = \begin{cases} F(\boldsymbol{k},\omega)\left(\sqrt{1+\frac{\varepsilon^c_{\boldsymbol{k}}}{E_{\boldsymbol{k}}}}\sqrt{(1+\frac{\varepsilon^s_{\boldsymbol{k}}}{E_{\boldsymbol{k}}}}\,\delta\left(\omega - E_{\boldsymbol{k}}\right)\right. & \\ \left. + \sqrt{1-\frac{\varepsilon^c_{\boldsymbol{k}}}{E_{\boldsymbol{k}}}}\sqrt{1-\frac{\varepsilon^s_{\boldsymbol{k}}}{E_{\boldsymbol{k}}}}\,\delta\left(\omega + E_{\boldsymbol{k}}\right)\right), & \text{for } |\omega| > |\varepsilon^c_{\boldsymbol{k}}|, \\ \frac{1}{\pi}\frac{D^c_+ D^s_+ D^c_- D^c_+ D^s_- D^s_+}{\left(D^c_- D^c_+ D^s_- D^s_+\right)^2 + \Delta^4_{\boldsymbol{k}}}, & \text{for } |\varepsilon^s_{\boldsymbol{k}}| < |\omega| < |\varepsilon^c_{\boldsymbol{k}}|, \\ 0, & \text{for } |\omega| < |\varepsilon^s_{\boldsymbol{k}}|\,, \end{cases} \tag{12}$$

where $D^{c,s}_{\pm} \equiv |\omega \pm \varepsilon^{c,s}(\boldsymbol{k})|^{1/2}$, and $F(\boldsymbol{k},\omega) \equiv \frac{1}{2}\frac{\Delta^2_{\boldsymbol{k}}}{(\varepsilon^c_{\boldsymbol{k}})^2 - (\varepsilon^s_{\boldsymbol{k}})^2}$. In this limit, the shape of the spectral density function is composed of two Dirac-delta peaks at $\sim \pm\Delta$, which correspond to the excitations across the gap, and of two wider bumps coming from the charge-spin separated parts of the total spectrum. The line is practically symmetric. For the case $\alpha \neq 0$ the spectral function has two sharp peaks and two small bumps in between. Then, the discrete pole structure due to the $\boldsymbol{k}$-independent Δ is smeared out, particularly when $\omega_c\delta \geq \Delta$.

In Fig. 3 we display the spectral intensity $S(\boldsymbol{k},\omega)$ describing the ARPES spectra [11] defined as

$$S(\boldsymbol{k},\omega) \sim \int d\omega' A(\boldsymbol{k},\omega') f(\omega') R(\omega' - \omega), \tag{13}$$

where $R(\omega - \omega')$ is the instrumental function, taken in a Gaussian form, with the dispersion $\tilde{\sigma} = 1$meV. The peaked structure appearing for $\Delta \neq 0$ is due to the pole at $|\omega| = E_{\boldsymbol{k}}$. The function is asymmetric (exhibits a long tail) at the large $|\omega|$, observed in the experiment [13,14]. This feature is not pronounced for $\alpha \to 0$ and poses a problem when one wants to reconcile observed asymmetry in the ARPES spectra with the linear resistivity in the whole temperature range. However, the scaling laws were derived assuming the linear dispersion relation, whereas $\rho(\omega)$ is derived taking a realistic $\varepsilon_{\boldsymbol{k}}$; this may be partly the source of differences. Also, the peak in $S(\boldsymbol{k},\omega)$ is not enhanced when the system transforms to SC phase. This discrepancy

with experiment may disappear if the Cooper-pair tunneling between the CuO_2 planes in SC phase is included, since then the system is effectively three-dimensional and the quasiparticles are well defined.

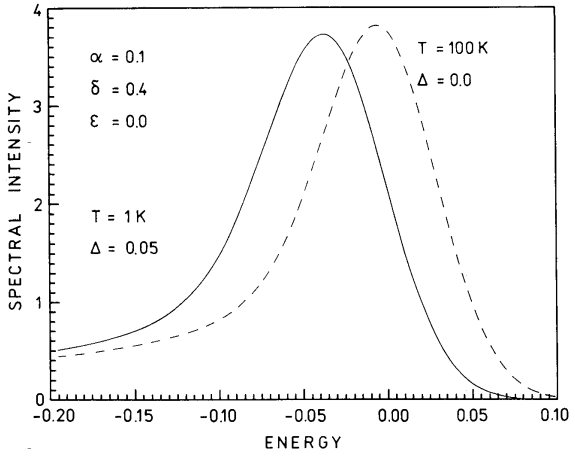

Fig. 3. Spectral intensity as a function of energy (for $\omega_c = 1\text{eV}$) for bare energy $\varepsilon_{\boldsymbol{k}} - \mu = 0$ in both normal ($\Delta = 0$) and superconducting ($\Delta = 0.05\,\text{eV}$) phases, as specified.

2.4. Tunneling conductivity

Integrating $A(\boldsymbol{k}, \omega)$ for $\Delta \neq 0$ over $\boldsymbol{k}$, we obtain the density of states shown in Fig. 4. The most striking feature is that the system has a pseudo gap even though we have taken *an isotropic gap parameter* $\Delta_{\boldsymbol{k}} \equiv \Delta$ in the computations. Also, the two parts are not generally symmetric. These properties of $\rho(\omega)$ are reflected in the single-particle tunneling. Namely, suppose the tunneling current is of the form

$$I = I_0 \int_{-\omega_c/2}^{\omega_c/2} d\xi_R \int_{-eV}^{0} d\xi_L \, A_R(\xi_R, \xi_L), \tag{14}$$

with $I_0 \equiv 2e|T|^2 \rho_L(0)$ being a constant. From the current we can obtain the conductance $G(V) = dI/dV$, which provides information about the density of states. In effect, for $\Delta \neq 0$ the conductance is nonzero at zero bias, and has a deep minimum that reflects the presence of the pseudo gap ($G(V) \sim \rho(\omega = eV)$). The behavior of the conductance ($G(V) = g_0 + g_1 V$) for small bias and the peak asymmetry reflect the results for various high-T_c superconductors [15].

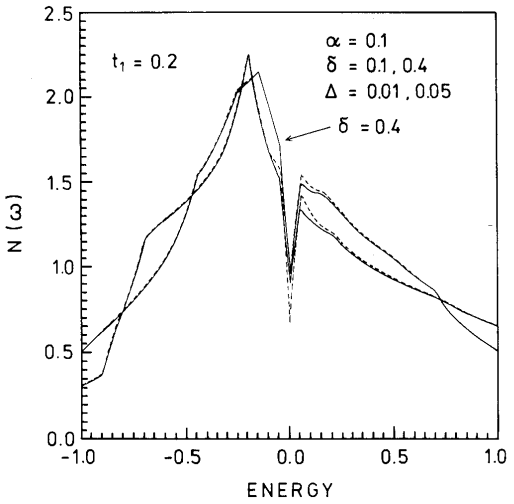

Fig. 4. Same as in Fig. 2 in SC phase for values of $\Delta = 10^{-2}$, and 5×10^{-2}, for $\delta = 0.1$ (full line) and $\delta = 0.4$ (dashed line).

2.5. The BCS self-consistent equation and the transition temperature

In accordance with the general scheme of BCS theory, one obtains the following self-consistent equation for the superconducting gap at nonzero temperature ($T > 0$)

$$\Delta_{\boldsymbol{k}} = \frac{1}{N} \sum_{\boldsymbol{k}'} V_{\boldsymbol{k}\boldsymbol{k}'} \Delta_{\boldsymbol{k}'} \chi_{\boldsymbol{k}'} \,, \tag{15}$$

where

$$\begin{aligned} \chi_{\boldsymbol{k}} \;=\; & \frac{1}{\pi} \int\limits_{\varepsilon^s_{\boldsymbol{k}}}^{\varepsilon^c_{\boldsymbol{k}}} d\omega \frac{x(\omega)\cos(\pi\alpha)\tanh(\beta\omega/2)}{(x(\omega)\sin(\pi\alpha)+|\Delta_{\boldsymbol{k}}|^2)^2+(x(\omega)\cos(\pi\alpha))^2} \\ & + \frac{1}{\pi} \int\limits_{\varepsilon^c_{\boldsymbol{k}}}^{\infty} d\omega \frac{x(\omega)\sin(2\pi\alpha)\tanh(\beta\omega/2)}{(x(\omega)\cos(2\pi\alpha)+|\Delta_{\boldsymbol{k}}|^2)^2+(x(\omega)\sin(2\pi\alpha))^2} \,, \end{aligned} \tag{16}$$

and

$$x(\omega) = \omega_c^{4\alpha} g^{-2}(\alpha) |\omega^2 - (\varepsilon^c_{\boldsymbol{k}})^2|^{\frac{1}{2}-\alpha} |\omega^2 - (\varepsilon^s_{\boldsymbol{k}})^2|^{\frac{1}{2}-\alpha}.$$

The self-consistent equation for $\Delta_{\boldsymbol{k}}$ has thus a nonstandard (non-Fermi liquid) form. This is due to the absence of the quasiparticle poles in the Luttinger–Green function. The contributions appearing in $\chi_{\boldsymbol{k}}$ derives from the cuts on the complex — ω plane.

The BCS limit of the above equation can be obtained in two steps. First, we must consider the $\alpha = 0$ limit. Then, the second term on the right hand side of the $\chi_{\boldsymbol{k}}$ expression gives the contribution with $\tanh(\frac{\beta E_k}{2})$ term because for small α the integrated function is a Dirac-delta function. However, the first term giving the contribution from the cut still survives. As a result, in the $\alpha \to 0$ limit we have

$$\chi_{\boldsymbol{k}} = \frac{1}{\pi} \int\limits_{\varepsilon^s_{\boldsymbol{k}}}^{\varepsilon^c_{\boldsymbol{k}}} d\omega \frac{x(\omega)\tanh(\beta\omega/2)}{(x(\omega))^2 + |\Delta_{\boldsymbol{k}}|^4} + \frac{|\Delta_{\boldsymbol{k}}|^2}{\sqrt{((\varepsilon^c_{\boldsymbol{k}})^2 + (\varepsilon^s_{\boldsymbol{k}})^2)^2 + 4|\Delta_{\boldsymbol{k}}|^4}} \frac{\tanh(\beta E_{\boldsymbol{k}}/2)}{E_{\boldsymbol{k}}}. \tag{17}$$

Finally, the BCS limit is recovered by putting $\varepsilon^c_{\boldsymbol{k}} = \varepsilon^s_{\boldsymbol{k}}$, since then

$$\chi_{\boldsymbol{k}} = \frac{1}{2E_{\boldsymbol{k}}} \tanh\left(\frac{\beta E_{\boldsymbol{k}}}{2}\right).$$

The value of the transition temperature is obtained by putting $\Delta_{\boldsymbol{k}} = 0$ in $\chi_{\boldsymbol{k}}$ and then solving again the self-consistent equation. Namely, taking the constant value of $N(0)$ for the density of states and assuming isotropic form of $V_{\boldsymbol{k}\boldsymbol{k}'} = V$ in the energy interval $[-\omega_D, \omega_D]$ around the Fermi energy, we obtain for $0 < \alpha < 1/4$ the expression

$$\frac{k_{\mathrm{B}}T_{\mathrm{c}}}{\omega_D} = \left[\frac{\cos(\pi\alpha)h_1(\alpha,\delta) + \sin(2\pi\alpha)h_2(\alpha,\delta) - 4\pi\alpha(\frac{\omega_{\mathrm{c}}}{\omega_D})^{4\alpha}\frac{1}{N(0)V}}{2(1-2^{1-4\alpha})\Gamma(4\alpha+1)\zeta(4\alpha)(\cos(\pi\alpha)k_1(\alpha,\delta) + \sin(2\pi\alpha)k_2(\alpha,\delta))}\right]^{\frac{1}{4\alpha}}, \tag{18}$$

where we defined the functions

$$\begin{aligned}
h_1 &= \int\limits_{1-\delta}^{1+\delta} dx((1+\delta)^2 - x^2)^{\alpha-1/2}(x^2 - (1-\delta)^2)^{\alpha-1/2}\,, \\
h_2 &= \int\limits_{1+\delta}^{\infty} dx(x^2 - (1+\delta)^2)^{\alpha-1/2}(x^2 - (1-\delta)^2)^{\alpha-1/2}\,, \\
k_1 &= \int\limits_{1-\delta}^{1+\delta} dx((1+\delta)^2 - x^2)^{\alpha-1/2}(x^2 - (1-\delta)^2)^{\alpha-1/2}x^{-4\alpha}\,, \\
k_2 &= \int\limits_{1+\delta}^{\infty} dx(x^2 - (1+\delta)^2)^{\alpha-1/2}(x^2 - (1-\delta)^2)^{\alpha-1/2}x^{-4\alpha}\,.
\end{aligned} \tag{19}$$

Examining the T_{c} expression we note that the T_{c} is nonzero only when the

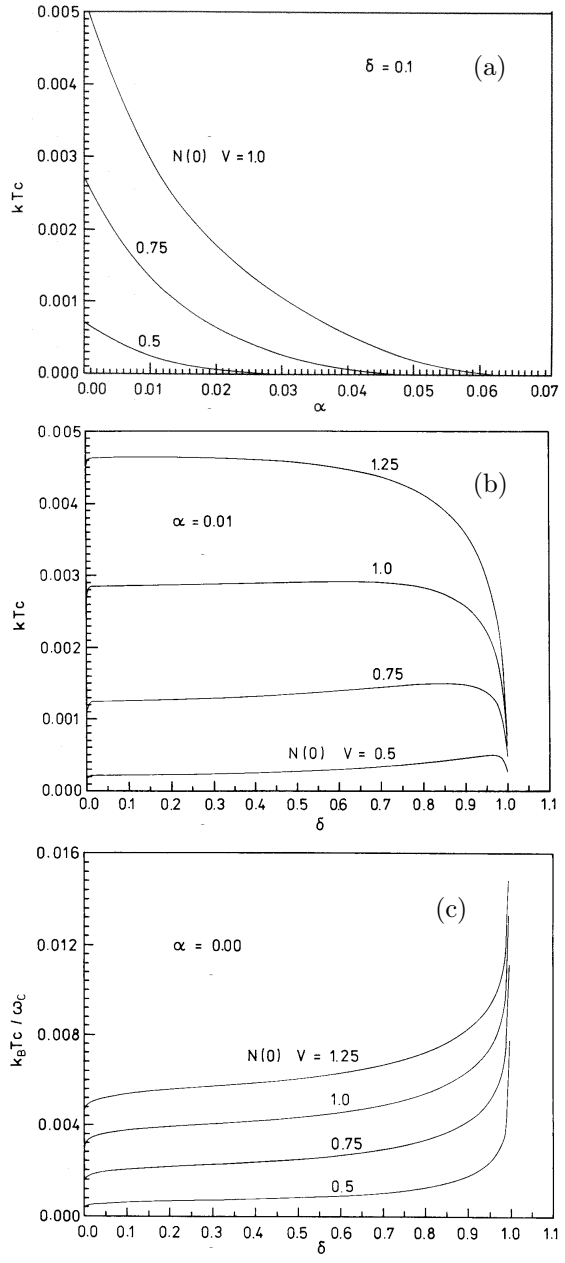

Fig. 5. Critical temperature T_c as a function of (a) α for $\delta = 0.01$, (b) δ for $\alpha = 0.01$, and (c) δ for $\alpha = 0$. Note the discontinuity in the T_c value when $\alpha \to 0$.

pairing potential exceeds a critical value given by

$$N(0)V_c = \frac{4\pi\alpha(\frac{\omega_c}{\omega_D})^{4\alpha}}{\cos(\pi\alpha)h_1 + \sin(2\pi\alpha)h_2}\,. \tag{20}$$

In the limit $\alpha = 0$ but $\delta \neq 0$ we obtain instead

$$k_{\mathrm{B}}T_{\mathrm{c}} = \hbar\omega_D \frac{2e^{\gamma}}{\pi} \exp\left(-\frac{\pi\gamma}{N(0)V} \frac{1}{K\left(\sqrt{1-(\frac{1-\delta}{1+\delta})^2}\right)} \right), \tag{21}$$

where $K(x)$ is the complete elliptic integral of the first kind. Numerical results are displayed in Figs. 5 (a)–(c), where both dependences on α and δ are displayed. From figure 5(a) it follows that T_{c} is a decreasing function of α and practically vanishes for $\alpha \sim 0.05$, depending on the value of $N(0)V$. On the contrary, a spectacular rise (and divergence) of T_{c} is observed in the limit $\alpha = 0$ and $\delta \to 1$, *i.e.* when $v_{\mathrm{F}}^s \to 0$. The physical origin of this divergence is not clear to us.

2.6. Ginzburg–Landau functional

One can also derive the Ginzburg–Landau free-energy functional within our model and for an isotropic form of the gap. It has the following form of $\alpha \neq 0$

$$\frac{1}{4m}\left(-i\nabla + \frac{2e\boldsymbol{A}}{c}\right)^2 \Psi + a\Psi + b \mid \Psi \mid^2 \Psi\,, \tag{22}$$

where

$$a = a'\left(1 - \left(\frac{T}{T_{\mathrm{c}}}\right)^{4\alpha}\right)\,, \tag{23}$$

and a' and b are complicated functions of α and δ. Thus the characteristic lengths $\lambda(T)$ and $\xi(T)$, as well as the critical magnetic field will have a nonstandard temperature dependence, with the power law scaling depending on the value of α. This functional is in the same class as that derived by Muthukumar *et al.* [16]. In the limit $\alpha = \delta = 0$ we obviously recover the standard form.

3. Concluding remarks

In the present contribution we have briefly summarized the results obtained for our choice of the Green function with branching cuts that possesses the two fundamental features of the Luttinger liquid: the anomalous scaling and the spin-charge separation. The two characteristics are accounted for

through the parameters α and δ. The results indicate clearly that the physical properties of the Luttinger liquid are significantly different from those of the Fermi liquid.

We should also emphasize that some of the properties of the high-temperature superconductors can be understood within this phenomenology, particularly those at the optimal doping (when $\alpha \to 0$), since then the dc resistivity $\rho \sim T$ and the value of T_c is maximal. However, to obtain a photoemission line enhancement as one crosses the superconducting transition with diminishing temperature, one requires a further analysis. Also, a transformation of the Luttinger liquid into the Fermi liquid should be studied carefully.

We are grateful to Prof. P.W. Anderson for useful comments.

REFERENCES

[1] L.D. Landau, *JEPT* **3**, 920 (1957); **5**, 101 (1957); **8**, 70 (1959); for review see: D. Pines, P. Nozieres, *Quantum Liquids*, vol.1, W.A. Benjamin 1966; G. Baym, C. Pethick, *Landau Fermi-Liquid Theory*, J. Wiley & Sons, Inc., New York 1991.

[2] *Windsurfing the Fermi Sea*, eds. T.T.S. Kuo, J. Speth, North-Holland, Amsterdam 1987.

[3] *High-Teperature Superconductivity* edited by K.S. Bedel *et al.*, Addison-Wesley, Reading, MA, 1990.

[4] C.M. Varma *et al.*, *Phys. Rev. Lett.* **63**, 1996 (1989).

[5] P.W. Anderson, *Phys. Rev. Lett.* **65**, 2306 (1990); *Phys. Rev.* **B55**, 11785 (1997); also: *The Theory of Superconductivity in the High-T_c Cuprates*, Princeton Univ. Press, 1997, where microscopic arguments for the ALL state are provided.

[6] P.W. Anderson, Y. Ren, in *The Normal State of High-T_c Superconductors: A New Quantum Liquid*, edited by K. Bedell *et al.*, Addison-Wesley, Reading, MA, 1990.

[7] M. Ogata, P.W. Anderson, *Phys. Rev. Lett.* **70**, 3087 (1993); P. Voruganti, A. Golubentsev, S. John, *Phys. Rev.* **B45**, 13945 (1992). We test this approximation by comparing the predicted scaling of resistivity with experiment (see below).

[8] L. Yin, S. Chakravarty, *Int. J. Mod. Phys.* **B10**, 805 (1996).

[9] K. Byczuk, J. Spałek, *Solid State Commun.* **99**, 99 (1996); *Phys. Rev.* **B51**, 7934 (1995).

[10] S. Chakravarty, A. Sudbø, P.W. Anderson, *Science* **261**, 337 (1993).

[11] The spectral density with $\alpha = 0$ has been obtained in $1d$ case *e.g.* in: J. Voit, *Phys. Rev.* **B47**, 6740 (1993).

[12] Z. Schlesinger, R. Collins, *Phys. Rev. Lett.* **65**, 801 (1990); J. Orenstein *et al.*, *Phys. Rev.* **B42**, 6342 (1990).

[13] D.S. Dessau *et al.*, *Phys. Rev. Lett.* **71**, 2781 (1993); K. Gofron *et al.*, *J. Phys. Chem. Solids* **54**, 1193 (1993).

[14] M. Randeira, J-C. Campuzano, preprint cond-mat 9709107.

[15] *Cf. e.g.* Z. Yusof, J.F. Zasadzinski, L. Coffey, preprint cond-mat 9709249.

[16] V.N. Muthukumar *et al.*, *Phys. Rev.* **B52**, 9647 (1995).